

# Noncanonical Wnt5a/JNK Signaling Contributes to the Development of D-Gal/LPS-Induced Acute Liver Failure

**Xiang-fen Ji**

Qilu Hospital of Shandong University Qingdao

**Yu-chen Fan**

Qilu hospital of Shandong University

**Fei Sun**

Qilu Hospital of Shandong University Qingdao

**Jing-wei Wang**

Qilu Hospital of Shandong University Qingdao

**kai wang** (✉ [wangdoc876@126.com](mailto:wangdoc876@126.com))

Qilu Hospital of Shandong University <https://orcid.org/0000-0002-6297-0147>

---

## Research Article

**Keywords:** acute liver failure, Wnt5a, c-jun N-terminal kinase, macrophage

**Posted Date:** October 21st, 2021

**DOI:** <https://doi.org/10.21203/rs.3.rs-995106/v1>

**License:**  This work is licensed under a Creative Commons Attribution 4.0 International License.

[Read Full License](#)

---

**Version of Record:** A version of this preprint was published at Inflammation on January 31st, 2022. See the published version at <https://doi.org/10.1007/s10753-022-01627-y>.

# Abstract

Acute liver failure (ALF) is a deadly clinical disorder with few effective treatments and unclear pathogenesis. In our previous study, we demonstrated that aberrant Wnt5a expression was involved in acute on chronic liver failure. However, the role of Wnt5a in ALF is unknown. We investigated the expression of Wnt5a and its downstream signaling of c-jun N-terminal kinase (JNK) in a mouse model of ALF established by co-injection of D-galactosamine (D-Gal) and lipopolysaccharide (LPS) in C57BL/6 mice. We also investigated the role of Box5, a Wnt5a antagonist *in vivo*. Moreover, the effect of Wnt5a/JNK signaling on downstream inflammatory cytokines expression, phagocytosis and migration in THP-1 macrophages was studied *in vitro*. Aberrant Wnt5a expression and JNK activation were detected in D-Gal/LPS-induced ALF mice. Box5 pretreatment reversed JNK activation, and eventually decreased the mortality rate of D-Gal/LPS-treated mice with reduced hepatic necrosis and apoptosis, serum ALT and AST levels, and liver inflammatory cytokines expression, although the last was not significant. We further demonstrated that recombinant Wnt5a (rWnt5a) induced tumor necrosis  $\alpha$  (TNF- $\alpha$ ) and Interleukin-6 (IL-6) mRNA expression, and increased the phagocytosis ability of THP-1 macrophages in a JNK-dependent manner, which could be restored by Box5. In addition, rWnt5a-induced migration of THP-1 macrophages was also turned by Box5. Our findings suggested that Wnt5a/JNK signaling play important role in the development of ALF, and Box5 could have particular hepatoprotective effects in ALF.

## Introduction

Acute liver failure (ALF) is a serious life-threatening syndrome characterized by abrupt hepatocyte necrosis, which results in altered coagulation and mentation [1]. Due to rapid progression to multiorgan failure and devastating complications, ALF is a disorder with high mortality and resource cost. Currently, the mainstay of ALF management is supportive care and liver transplantation [2]. Unfortunately, few disease-specific or general interventions are available to improve outcomes in supportive system [3]. Although liver transplantation is the determined cure for ALF, extensions are challenged by availability of suitable organs, high costs and sufferings from the rejection after transplantation. Going even further, the pathogenesis of ALF is complicated and remains unclear. Nevertheless, it is generally believed that ALF is associated with direct cellular damage caused by viruses, drugs and other uncommon sources, as well as more importantly, immune-mediated inflammatory injury [4, 5]. Furthermore, many studies indicated that the dysfunction of monocytes and macrophages along with their induced inflammatory cytokines play significant roles in the initiation and progression of ALF [6, 7].

Wnt proteins are a large family of secreted glycoproteins, which participate in multiple cellular processes, such as cell proliferation, differentiation, migration, polarization, and apoptosis [8, 9]. Aberrant Wnt signaling has been demonstrated in many human diseases, ranging from cancer to metabolic diseases [10, 11]. Recently, increasing researches began to focus on the involvement of noncanonical Wnt, particularly Wnt5a, in inflammation [9, 12, 13]. Wnt5a expression was observed upregulated in sera of patients with sepsis, and it induced the expression of pro-inflammatory cytokines in macrophages in response to microbial stimulation [14–16]. Moreover, suppression of Wnt5a signaling impaired

macrophages clearance of bacterial infection both in vitro and in vivo [17]. As a noncanonical Wnt, Wnt5a can activate c-jun N-terminal kinase (JNK) signaling in inflammatory processes [12, 18]. JNK is a stress-activated kinase in the mitogen activated protein kinase (MAPK) family. Activated JNK was demonstrated mediating the hepatotoxic effects in ALF [19, 20]. Regulation of JNK signaling shed new light on the treatment of ALF [21].

In our previous study, we suggested that Wnt5a expression in sera and peripheral blood mononuclear cells (PBMCs) of patients with acute on chronic hepatitis B liver failure (ACHBLF) was significantly increased, and the higher level of Wnt5a, the worse prognosis they had [22]. However, the role of Wnt5a, especially Wnt5a/JNK signaling in ALF has not been studied. The experimental ALF model induced by D-galactosamine plus lipopolysaccharide (D-Gal/LPS) has been extensively studied to explore the pathogenesis and to test potential therapeutics for ALF [23]. In this study, we aimed to investigate the role of Wnt5a/JNK signaling and its antagonist Box5 in ALF with the use of D-Gal/LPS-induced ALF model and THP-1 cells.

## Materials And Methods

### Animals

The male C57BL/6 mice (6-8 weeks old, weighing 18-25g) were purchased from Pengyue laboratory animal breeding Co. Ltd. (Jinan, China). All mice were housed under controlled conditions with a standard temperature and humidity, 12 hours of light-dark circulation, and had free access to food and water. LPS was purchased from Solarbio and D-Gal was from aladdin, and they were dissolved in sterile normal saline (NS). Firstly, mice were randomly divided into Control group (n=10) and D-Gal/LPS group (n=10). Mice in the D-Gal/LPS group received a combination of D-Gal (500mg/kg) with LPS (10ug/kg) intraperitoneally, while mice in Control group received NS only. Five hours later, the mice were sacrificed to obtain liver tissues and blood samples. Secondly, to investigate the hepatoprotective effect of Box5, other sixty mice were randomly divided into NS group (n=30) and Box5 group (n=30). The mice were injected with Box5 (1mg/kg; Box5 group) or NS (NS group) intraperitoneally one hour before D-Gal/LPS administration. In detail, twenty mice in each group were monitored for 72h after D-Gal/LPS administration for the survival analysis, and ten mice in each group were sacrificed five hours after D-Gal/LPS administration for other experiments. All animal experiments were approved by the Ethical Committee of Qilu hospital (Qingdao), Shandong University.

### Cell culture

Human monocyte cell line THP-1 was purchased from Chinese Academy of Medical Sciences and was cultured in RPMI 1640 medium supplemented with 10% fetal bovine serum (FBS). THP-1 cells were induced to differentiate into macrophages by incubation with 100nM phorbol 12-myristate 13-acetate (PMA, Selleckchem) for 24h. To investigate the effect of Wnt5a on THP-1 macrophages, different concentrations (50, 100, 500ng/ml) of recombinant Wnt5a (rWnt5a, R&D systems) were added to the medium of THP-1 macrophages with different expose periods (1, 3, 6h).

# Histology staining, immunohistochemistry and double labeling immunofluorescence staining

Fresh liver tissues were fixed in 10% neutral-buffered formalin, embedded in paraffin, and sectioned at 4µm thickness. Deparaffinized sections stained with haematoxylin and eosin (H&E) were evaluated under a light microscope for histological examination. Additionally, the sections were incubated with primary antibody against Wnt5a (1:100; Bioss), followed by incubation with horseradish peroxidase (HRP)-labeled secondary antibody for immunohistochemistry staining. Target proteins were stained with diaminobenzidine (DAB) and evaluated under a light microscope. For double labeling immunofluorescence staining, sections were firstly incubated with primary antibody against F4/80 (1:3000; Servicebio) overnight, and incubated with fluorochrome-conjugated secondary antibodies the next day. Subsequently, sections were incubated with the second primary antibody against Wnt5a (1:200; Bioss) overnight, and stained with fluorochrome-conjugated secondary antibodies on the third day. Nucleus staining was conducted using 4', 6-diamidino-2-phenylindole (DAPI). The fluorescent images were captured under a fluorescence microscope.

## Analysis of apoptosis

Apoptosis was analyzed using One Step TdT-mediated dUTP Nick-End Labeling (TUNEL) Apoptosis Assay Kit (Beyotime) according to the manufacturer's suggestions. Sections were deparaffinized and treated with 20µg/ml proteinase K for 30min at 37°C, and then washed for three times. Subsequently, these sections were darkly incubated with TUNEL reaction for 1h at 37°C. At last, fluorescence-labeled images were visualized under a fluorescence microscopy.

## Liver function assays

Blood samples were taken from the heart of the mice and centrifuged at 3000rpm for 10min to separate serum. Liver function markers of alanine aminotransferase (ALT) and aspartate aminotransferase (AST) were analyzed by microplate assay using the corresponding determination kits (Nanjing Jiancheng Bioengineering Institute, Nanjing, China) according to the manufacturer's instructions.

## RNA extraction and Quantitative Real-Time PCR (qPCR)

Total RNA was extracted from liver tissues and cells using Trizol and was reverse transcribed into cDNA by using RevertAid First Strand cDNA Synthesis Kits (Thermo Fisher Scientific). qPCR was performed using Blaze Taq<sup>TM</sup> SYBR® Green qPCR Mix 2.0 (GeneCopoeia). Target gene expression was normalized with reference to GAPDH. Primer sequences for qPCR amplification are shown in Table 1.

Table 1  
Primers for real-time PCR

Primers	Sequences
Human wnt5a	5'-GTCTTGAGCTTGGGC-3' 5'-ACGTCCATGTCTATAACGA-3'
Human IL-6	5'-AGCCACTCACCTCTTCAGAAC-3' 5'-GCCTCTTTGCTGCTTTCACAC-3'
Human IL-1 $\beta$	5'-GTGGCAATGAGGATGACTTGTTTC-3' 5'-TAGTGGTGGTCGGAGATTCGTA-3'
Human TNF- $\alpha$	5'-CTGCTGCACTTTGGAGTGAT-3' 5'-GATGATCTGACTGCCTGGG-3'
Human IL-10	5'-ATGCTTCGAGATCTCCGAGA-3' 5'-AAATCGATGACAGCGCCGTA-3'
Human GAPDH	5'-GCACCGTCAAGGCTGAGAAC-3' 5'-TGGTGAAGACGCCAGTGGA-3'
Mice wnt5a	5'-GAATCCCATTTGCAACCCCTCACC-3' 5'-GCTCCTCGTGTACATTTTCTGCCC-3'
Mice IL-6	5'-TTCCATCCAGTTGCCTTCTT-3' 5'-CAGAATTGCCATTGCACAAC-3'
Mice IL-1 $\beta$	5'-GAAATGCCACCTTTTGACAGTG-3' 5'-TGGATGCTCTCATCAGGACAG-3'
Mice TNF- $\alpha$	5'-TCTTCTCATTCTGCTTGTGG-3' 5'-CACTTGGTGGTTTGCTACGAC-3'
Mice IL-10	5'-CTTACTGACTGGCATGAGGATCA-3' 5'-GCAGCTCTAGGAGCATGTGG-3'
Mice GAPDH	5'-CCATGTTTCGTCATGGGTGTGAACCA-3' 5'-GCCAGTAGAGGCAGGGATGATGTTTC-3'
IL-6: Interleukin-6; IL-1 $\beta$ : Interleukin-1 $\beta$ ; TNF- $\alpha$ : tumor necrosis $\alpha$ ; IL-10: Interleukin-10.	

## Western blot Analysis

To extract total proteins, liver tissues and cells were homogenized in cold RIPA with phenyl methane sulfonyl fluoride (PMSF) protease inhibitor and phosphatase inhibitor. Protein concentrations were determined by the Bicinchoninic Acid (BCA) Protein Assay Kit (Sparkjade). Equal protein samples were separated by SDS-PAGE, transferred onto the PVDF membranes, and incubated with primary antibodies against Wnt5a (1:250; R&D systems), JNK (1:1000; Cell Signaling Technology), phospho-JNK (p-JNK; 1:1000; Cell Signaling Technology), and  $\beta$ -actin (1:1000; Cell Signaling Technology). After stained with HRP-conjugated secondary antibody, protein bands were visualized using the ECL super Kit (Sparkjade).

## Migration assay

Cell migration was evaluated using 24-well transwells with 8.0 $\mu$ m pore polycarbonate membrane inserts. About  $1 \times 10^5$  THP-1 cells were suspended in 100 $\mu$ L serum-free PRIM 1640 medium containing PMA and rWnt5a with different concentrations (50, 100, 500ng/ml). Cells were seeded in the upper chamber, and 600 $\mu$ L medium containing 20% FBS was added to the lower chamber. After incubation for 24h, the cells that have migrated to the underside of the upper chamber were fixed in paraformaldehyde and stained with crystal violet. Cell images were visualized under an inverted microscope.

## Phagocytosis assay

Neutral red uptake assay was used to measure the phagocytic ability of THP-1 macrophages. After induced by PMA for 24h, the cells were cultured with rWnt5a for 1h, 3h and 6h with various concentrations (50, 100, 500ng/ml). Then, 100 $\mu$ L natural red (0.1%, Solarbio) was added to the cells and incubated at 37°C. Two hours later, the cells were washed three times and lysed overnight at 4°C by a 200 $\mu$ L mixture of anhydrous ethanol and acetic (the volume ratio of them was 1:1). Finally, the optical density value read at 550 nm represent the phagocytic ability of THP-1 macrophages.

## Statistical analysis

Data were expressed as mean  $\pm$  standard error of mean (SEM). Differences were determined by two tailed Student's t-test or one-way analysis of variance. Statistical analysis were performed and presented using Prism GraphPad 5.0 software. A *P* value less than 0.05 was considered statistically significant.

## Results

### Hepatic damage caused by D-Gal/LPS administration

With the use of H&E and TUNEL staining, we found that hepatocellular necrosis and apoptosis occurred more in the mice of D-Gal/LPS group than that in Control group (Fig. 1a and 1b). Serum ALT and AST, as typical markers of liver damage, were significantly elevated in D-Gal/LPS treated mice compared to those in Control group ( $P < 0.05$ ; Fig. 1c). Additionally, the mRNA levels of tumor necrosis  $\alpha$  (TNF- $\alpha$ ), Interleukin-6 (IL-6), Interleukin-1 $\beta$  (IL-1 $\beta$ ) and Interleukin-10 (IL-10) in liver tissues of mice in D-Gal/LPS group were increased compared to those in Control group ( $P < 0.05$  for all; Fig. 1d).

# Aberrant Wnt5a expression and JNK activation in liver tissues induced by D-Gal/LPS

To investigate the expression of Wnt5a in liver tissues, we firstly detected Wnt5a protein levels by immunohistochemistry staining. As shown in Fig. 2a, remarkable upregulation of Wnt5a expression was discovered in D-Gal/LPS group compared to that in Control group, which was further confirmed by quantitative analysis for immunohistochemistry staining ( $P < 0.05$ ; Fig. 2b). Additionally, we observed that liver Wnt5a was primarily expressed in the necrotic area but not on viable hepatocytes, where were infiltrated lots of macrophages. To determine the correlation between the Wnt5a expression and macrophages, we explored the co-localization of Wnt5a and F4/80 (a pan-macrophage marker) at liver sections of the mice in Control and D-Gal/LPS group using double labeling immunofluorescence staining. The results in Fig. 2c indicated that Wnt5a was primarily co-expressed with F4/80.

Interestingly, two distinct protein bands of Wnt5a were detected when we further validated our findings by Western blot. Notably, the intensities of the upper band ( $\sim 58\text{kDa}$ ) were increased in mice of D-Gal/LPS group ( $P < 0.05$ ), whereas the expression of the lower band ( $\sim 43\text{kDa}$ ) had no significant difference compared with those in Control group ( $P > 0.05$ ; Fig. 2d). However, just to make matters more interesting, the mRNA expression of Wnt5a tend to be significantly decreased in mice of D-Gal/LPS group compared with that in Control group ( $P < 0.05$ ; Fig. 2e). To investigate JNK activation in D-Gal/LPS treated mice, we performed Western blot with antibodies of p-JNK (activated JNK) and JNK (total JNK). As shown in Fig. 2f, mice in D-Gal/LPS group showed higher levels of p-JNK/JNK ratio than those in Control group ( $P < 0.05$ ).

## Hepatoprotective effect of Box5 by inhibiting Wnt5a/JNK signaling

To gain insight of Wnt5a signaling in ALF, we evaluated the effect of Wnt5a inhibition with its antagonist, Box5. As shown in Fig. 3a, Box5 efficiently alleviated hepatocyte necrosis, hepatic hemorrhage, and restored the liver structure. In addition, TUNEL positive cells (Fig. 3b) and liver damage markers of ALT and AST ( $P < 0.05$ ;  $P < 0.05$ ; Fig. 3c) were also reduced by Box5. We further analyzed survival rates of mice in Box5 group and NS group. As indicated in Fig. 3d, the survival rate of the mice in Box5 group was significantly lower than that in NS group ( $P < 0.05$ ). However, although the mRNA expression of inflammatory cytokines such as IL-1 $\beta$ , IL-6, TNF- $\alpha$  and IL-10 was tend to decrease in mice pretreated with Box5 compared with that in mice given NS, the difference was not significant ( $P > 0.05$  for all; Fig. 3e). To know more about JNK signaling, we further detected whether Box5 pretreated mice show lower JNK activation. Results suggested that liver p-JNK/JNK ratio in mice of Box5 group was reduced compared with that of NS group ( $P < 0.05$ ; Fig. 3f).

## Mediations on downstream genes, migration and phagocytosis of THP-1 macrophages by rWnt5a

To evaluate the effects of exogenous Wnt5a in vitro, we incubated THP-1 macrophages with rWnt5a at different concentrations or durations. Within a 6h period, the mRNA expression of TNF- $\alpha$  and IL-6 was detected distinctly increased at 1h in THP-1 macrophages treated with 50ng/ml rWnt5a ( $P<0.05$ ;  $P<0.05$ ; Fig. 4a). However, no significant difference was detected in the mRNA expression of IL-1 $\beta$  and IL-10 ( $P>0.05$ ;  $P>0.05$ ; Fig. 4a). Subsequently, we investigated whether cellular functions like migration and phagocytosis were affected by rWnt5a. As shown in Fig. 4b and Fig. 4c, we found that the migratory ability of THP-1 macrophages was remarkably improved by incubation with rWnt5a for 24h, especially they incubated with 50 or 100ng/ml rWnt5a ( $P<0.05$ ). Moreover, the phagocytic ability (A550nm) of THP-1 macrophages was also significantly enhanced when they were exposed to 100ng/ml rWnt5a for 1 hour ( $P<0.05$ ; Fig. 4d). However, no significant differences of phagocytosis were detected among cells incubated with 50 or 500ng/ml rWnt5a within a 6-hour duration ( $P>0.05$  for all; Fig. 4d). Finally, we detected the JNK signaling in THP-1 macrophages treated by rWnt5a. Activated JNK rapidly reached maximum in an hour in THP-1 macrophages induced by 50ng/ml rWnt5a ( $P<0.05$ ; Fig. 4e), and higher JNK activation was also investigated in THP-1 macrophages treated by 50 or 100ng/ml rWnt5a for an hour compared with that in cells treated by 500ng/ml rWnt5a or untreated cells ( $P<0.05$  for all; Fig. 4f).

## Most effects exerted by rWnt5a on THP-1 macrophages reversed by Box5 and SP600125

In order to know better of the Wnt5a/JNK signaling in vitro, we investigated whether inflammatory cytokines expression, phagocytosis and migration of THP-1 macrophages induced by rWnt5a could be reversed by Box5 and a specific JNK inhibitor, SP600125. Data suggested that rWnt5a-induced JNK activation was blocked by 200 $\mu$ M Box5 ( $P<0.05$ ; Fig. 5a) and 40nM SP600125 ( $P<0.05$ ; and Fig. 5b). In contrast to robust upregulation induced by rWnt5a, Box5 and SP600125 remarkably restored the increased mRNA expression of IL-6 and TNF- $\alpha$  ( $P<0.05$ ;  $P<0.05$ ; Fig. 5c and Fig. 5d). Moreover, Wnt5a-enhanced phagocytosis of THP-1 macrophages was also turned back by Box5 ( $P<0.05$ ; Figure 5e) and SP600125 ( $P<0.05$ ; Fig. 5f). Finally, as shown in Fig. 5g and Fig. 5i, the improved migration ability of THP-1 macrophages induced by rWnt5a was also reversed after co-incubation with Box5 ( $P<0.05$ ). However, SP600125 had no effect on rWnt5a-induced migration of THP-1 macrophages ( $P<0.05$ ; Fig. 5h and Fig. 5j).

## Discussion

In our study, it indicated that aberrant Wnt5a expression and JNK activation were detected in a mouse ALF model induced by D-Gal/LPS. In vivo, pretreatment of Box5, a Wnt5a antagonist, restored JNK activation, and exactly attenuated D-Gal/LPS-induced liver injury, as indicated by changes in liver pathology and ALT/AST levels, as well as decreased the mortality rate. In vitro, we demonstrated that downstream inflammatory cytokines expression and phagocytosis of THP-1 macrophages induced by rWnt5a were dependent on JNK activation, which could be reversed by Box5. In addition, rWnt5a-induced migration of THP-1 macrophages was also turned by Box5.

ALF is a deadly clinical disorder characterized by overwhelming hepatocyte death and rapid deterioration of normal liver function. Central to the pathogenesis of ALF is dysfunction of inflammation and immune response to various causes, which in turn exacerbates hepatocellular necrosis and apoptosis [24, 25]. ALF induced by D-Gal/LPS has been widely used as an animal model to elucidate pathogenesis and evaluate the efficiency of hepatoprotective agents [23, 26]. LPS, part of outer membrane of gram-negative bacteria, can greatly stimulate secretion of pro-inflammatory cytokines, such as IL-1 $\beta$ , IL-6 and TNF- $\alpha$  [27]. D-Gal, a specific hepatotoxic agent, can greatly increase hepatocellular death by enhancing their sensitivity to inflammatory injury [28]. Resembling human ALF, co-injection of D-Gal and LPS into mice in our study resulted in large liver necrotic foci, increased hepatocellular apoptosis, loss of liver function and elevated expression of inflammatory cytokines.

Since it was first reported that cytokines such as IL-6, Interleukin-8 (IL-8), and Interleukin-15 (IL-15) were upregulated by Wnt5a in rheumatoid arthritis synovial fibroblasts [29], there has been huge interest in Wnt5a signaling in inflammatory process. A subsequent study indicated that Wnt5a promotes Interleukin-12 (IL-12) synthesis and enhances the inflammation of human mononuclear cells induced by microbial stimulation [15]. Consistent with another research indicating that Wnt5a was upregulated in sera of patients with sepsis [14], our previous study showed that serum Wnt5a was increased in patients with ACHBLF compared with that in patients with CHB and healthy controls [22]. In our present study, we also suggested that liver Wnt5a protein expression was significantly elevated in mice of D-Gal/LPS group contrast to that in Control group by immunohistochemistry. However, two forms of Wnt5a with distinct molecular weights were detected in liver tissues, when we further determined our results by Western blot. We observed an increase in the bigger molecular weight of Wnt5a (~58 kDa) in mice with D-Gal/LPS administration. Similar findings that Wnt5a has two or more forms in one tissue have been observed in murine lung tissue [30] and neuron [31], although their Wnt5a were detected with different molecular weights from ours. Wnt proteins heavily rely on posttranslational modifications, such as glycosylation and palmitoylation, to secret and function, and they can also agglomerate into multimeric or oligomerized complexes [32, 33]. Perhaps, it partly explains our results, which undoubtedly needs further in-depth study to confirm. To get more insight of Wnt5a in ALF, we also evaluate the Wnt5a transcription by qPCR. Interestingly, Wnt5a mRNA expression in liver tissues of mice in D-Gal/LPS group was decreased compared with that in Control group, just opposite to its protein pattern. This contradictory expression of Wnt5a transcription and translation in liver tissue of D-Gal/LPS mice was similar to that observed in hepatocellular carcinoma and para-carcinoma liver tissues [34]. Thus, we speculated that some unclear mechanisms remain in the regulation of Wnt5a protein expression except posttranslational modifications, which exactly requires us to explore in the future. Nevertheless, these data suggested that Wnt5a signaling was involved in the development of ALF.

To determine the potential role of Wnt5a in ALF, we evaluate the effect of Wnt5a inhibition on the development of ALF with its antagonist, Box5. Box5 has been described to be a competitive inhibitor of Wnt5a through binding to its receptor to inhibit the biological activity of Wnt5a signaling [35]. Our results in the present study clearly showed that Wnt5a inhibition by Box5 alleviated pathologic severity, ameliorated liver function, and decreased mortality rate of ALF mice. In addition, Box5 pretreatment could

also reduce the stimulation of inflammatory cytokines, like IL-1 $\beta$ , IL-6, TNF- $\alpha$  and IL-10 induced by D-Gal/LPS, although not significant. These results were consistent with those in diabetic nephropathy suggested by Li and et al [36]. Taken together, it indicated that Wnt5a inhibition by Box5 could be a potential therapeutic strategy for ALF.

Noncanonical Wnt5a signaling comprises two main pathways: Wnt5a/Ca<sup>2+</sup> pathway and the Wnt5a/JNK or planar cell polarity (PCP) pathway [37]. Therein JNK signaling was widely demonstrated to be involved in inflammation [36, 38, 39]. Activated JNK participated in stimulation of many inflammatory cytokines by LPS [39, 40]. Phosphorylation of JNK mediated hepatotoxicity in acetaminophen-induced ALF [20]. Moreover, by attenuating JNK-mediated mitochondrial translocation, D-Gal/LPS-induced ALF could be ameliorated [41]. JNK inhibition with two different JNK inhibitors in vivo markedly reduced hepatic necrosis and apoptosis in paracetamol-induced ALF [42]. In this regard, we focused on JNK signaling as the downstream pathway of Wnt5a in our present research. As we expected, activated JNK was detected in liver tissues of mice in D-Gal/LPS group, and restored by Box5 pretreatment. In summary, results manifested that Wnt5a/JNK signaling play an important role in presence and progression of ALF.

Basal Wnt5a expression was observed in PBMC, PBMC-derived macrophage, alveolar macrophage, microglia and macrophage cell lines [12]. We found that Wnt5a was overexpressed on liver macrophages rather than hepatocytes. Dysfunction of monocyte and macrophage is central to ALF development [6]. As is widely known, it is necessary for the initiation and propagation of ALF that liver macrophages recognize and phagocyte pathogens or debris and stimulate inflammatory cytokines expression, as well as monocytes are recruited to differentiate into macrophages to expand the macrophage pool and promote tissue destruction. Considering above aspects, we explored the role of Wnt5a/JNK signaling in activation of THP-1 macrophages in vitro, which originally exist as one of monocyte cell lines, but was induced to differentiate into macrophage by PMA in our study. Results indicated that rWnt5a could induce increased mRNA expression of TNF- $\alpha$  and IL-6, and enhance the phagocytosis and migration abilities of THP-1 macrophages. These cellular regulations were dependent on JNK signaling except migration, as the JNK inhibitor, SP600125 totally abolished them. Box5 not only restored the above modulations of THP-1 macrophages but also blocked the activation of JNK induced by rWnt5a. To sum up, our findings supported that JNK signaling participated in the regulation of macrophages and Wnt5a was a regulator of JNK signaling. Furthermore, Wnt5a/JNK signaling participated in the development of ALF probably by regulating the activation of macrophages.

There are some limitations in our present study. One is that the mechanism under the contradictory expression of Wnt5a mRNA and protein expression remains unclear. Since our study focused more on the function of Wnt5a protein, more researches concerned on the regulation of transcription and translation are needed in the future. Another one is that the Wnt5a-knockout mice model is deserved to be the most accurate experimental tool to investigate its function. Unfortunately, homozygous Wnt5a-knockout mice exhibit perinatal lethality, due to developmental defects [43] and mice with Wnt5a-siRNA may not be blocked in liver Wnt5a protein expression, as suggested by our above results. Therefore, we selected

Box5, stated as a Wnt5a antagonist, to inhibit Wnt5a protein in mice. If the more insight of Wnt5a is further determined, conditional Wnt5a-knock out mice model may be the best option in future researches.

In conclusion, our findings provide strong evidence that aberrant Wnt5a/JNK signaling mediated massive hepatocellular necrosis and apoptosis, increased serum ALT and AST, and elevated inflammatory cytokines expression in D-Gal/LPS-induced ALF mice. Box5, as wnt5a antagonist could efficiently abolish these mediations and eventually improved the outcomes of D-Gal/LPS-induced ALF mice. Moreover, Wnt5a, expressed primarily on liver macrophages, was demonstrated to induce the activation of THP-1 macrophages in a JNK-dependent manner, which were also reversed by Box5. Overall, our results supported that Wnt5a/JNK signaling was involved in the development of ALF, partly via the regulation of macrophages and Box5 may be a potential effective agent for the treatment of ALF.

## Declarations

### AUTHORS' CONTRIBUTIONS

Xiang-Fen Ji designed the study, carried out the experiments and wrote the first draft of the manuscript. Fei Sun performed some experiments. Jing-Wei Wang analyzed some data. Yu-Chen Fan analyzed some data and involved in editing the manuscript. Kai Wang revised it critically for important intellectual content.

### FOUNDING

This work was supported by the National Natural Science Foundation of China (81970522), Shandong University multidisciplinary research and innovation team of young scholars (2020QNQT11), China Postdoctoral Science Foundation (2020M672074) and Scientific Research Foundation of Qilu Hospital of Shandong University (Qingdao) (QDKY2017QN13).

### DATA AVAILABILITY

All data generated or analyzed during the study are included in this published article.

**Ethics Approval.** All animal experiments were approved by the Ethical Committee of Qilu hospital (Qingdao), Shandong University.

**Consent to Participate.** Not applicable.

**Consent for Publication.** Not applicable.

**Conflict of interest.** The authors declare that they have no conflict of interest.

## References

1. Stravitz, R. T., and W. M. Lee. 2019. Acute liver failure. *Lancet* 394: 869–881.

2. Khan, R., and S. Koppe. 2018. Modern Management of Acute Liver Failure. *Gastroenterol Clin North Am* 47: 313–326.
3. Reuben, A., H. Tillman, R. J. Fontana, T. Davern, B. McGuire, R. T. Stravitz, V. Durkalski, A. M. Larson, I. Liou, O. Fix, M. Schilsky, T. McCashland, J. E. Hay, N. Murray, O. S. Shaikh, D. Ganger, A. Zaman, S. B. Han, R. T. Chung, A. Smith, R. Brown, J. Crippin, M. E. Harrison, D. Koch, S. Munoz, K. R. Reddy, L. Rossaro, R. Satyanarayana, T. Hassanein, A. J. Hanje, J. Olson, R. Subramanian, C. Karvellas, B. Hameed, A. H. Sherker, P. Robuck, and W. M. Lee. 2016. Outcomes in Adults With Acute Liver Failure Between 1998 and 2013: An Observational Cohort Study. *Ann Intern Med* 164: 724–732.
4. Grek, A., and L. Arasi. 2016. Acute Liver Failure. *AACN Adv Crit Care* 27: 420–429.
5. Dong, V., R. Nanchal, and C. J. Karvellas. 2020. Pathophysiology of Acute Liver Failure. *Nutr Clin Pract* 35: 24–29.
6. Triantafyllou, E., K. J. Woollard, M. J. W. McPhail, C. G. Antoniades, and L. A. Possamai. 2018. The Role of Monocytes and Macrophages in Acute and Acute-on-Chronic Liver Failure. *Frontiers in immunology* 9: 2948.
7. Possamai, L. A., M. R. Thursz, J. A. Wendon, and C. G. Antoniades. 2014. Modulation of monocyte/macrophage function: a therapeutic strategy in the treatment of acute liver failure. *Journal of hepatology* 61: 439–445.
8. Logan, C. Y., and R. Nusse. 2004. The Wnt signaling pathway in development and disease. *Annual review of cell and developmental biology* 20: 781–810.
9. George, S. J. 2008. Wnt pathway: a new role in regulation of inflammation. *Arteriosclerosis, thrombosis, and vascular biology* 28: 400–402.
10. Nusse, R., and H. Clevers. 2017. Wnt/ $\beta$ -Catenin Signaling, Disease, and Emerging Therapeutic Modalities. *Cell* 169: 985–999.
11. Zhan, T., N. Rindtorff, and M. Boutros. 2017. Wnt signaling in cancer. *Oncogene* 36: 1461–1473.
12. Shao, Y., Q. Zheng, W. Wang, N. Xin, X. Song, and C. Zhao. 2016. Biological functions of macrophage-derived Wnt5a, and its roles in human diseases. *Oncotarget* 7: 67674–67684.
13. Sessa, R., D. Yuen, S. Wan, M. Rosner, P. Padmanaban, S. Ge, A. Smith, R. Fletcher, A. Baudhuin-Kessel, T. P. Yamaguchi, R. A. Lang, and L. Chen. 2016. Monocyte-derived Wnt5a regulates inflammatory lymphangiogenesis. *Cell research* 26: 262–265.
14. Pereira, C., D. J. Schaer, E. B. Bachli, M. O. Kurrer, and G. Schoedon. 2008. Wnt5A/CaMKII signaling contributes to the inflammatory response of macrophages and is a target for the antiinflammatory action of activated protein C and interleukin-10. *Arteriosclerosis, thrombosis, and vascular biology* 28: 504–510.
15. Blumenthal, A., S. Ehlers, J. Lauber, J. Buer, C. Lange, T. Goldmann, H. Heine, E. Brandt, and N. Reiling. 2006. The Wingless homolog WNT5A and its receptor Frizzled-5 regulate inflammatory responses of human mononuclear cells induced by microbial stimulation. *Blood* 108: 965–973.
16. Nanbara, H., N. Wara-aswapati, T. Nagasawa, Y. Yoshida, R. Yashiro, Y. Bando, H. Kobayashi, J. Khongcharoensuk, D. Hormdee, W. Pitiphat, J. A. Boch, and Y. Izumi. 2012. Modulation of Wnt5a

- expression by periodontopathic bacteria. *PloS one* 7: e34434.
17. Jati, S., S. Kundu, A. Chakraborty, S. K. Mahata, V. Nizet, and M. Sen. 2018. Wnt5A Signaling Promotes Defense Against Bacterial Pathogens by Activating a Host Autophagy Circuit. *Frontiers in immunology* 9: 679.
  18. Che, C., C. Li, J. Lin, J. Zhang, N. Jiang, K. Yuan, and G. Zhao. 2018. Wnt5a contributes to dectin-1 and LOX-1 induced host inflammatory response signature in *Aspergillus fumigatus* keratitis. *Cellular signalling* 52, 103-111.
  19. Seki, E., D. A. Brenner, and M. Karin. 2012. A liver full of JNK: signaling in regulation of cell function and disease pathogenesis, and clinical approaches. *Gastroenterology* 143: 307–320.
  20. Torres, S., A. Baulies, N. Insausti-Urkia, C. Alarcón-Vila, R. Fucho, E. Solsona-Vilarrasa, S. Núñez, D. Robles, V. Ribas, L. Wakefield, M. Grompe, M. I. Lucena, R. J. Andrade, S. Win, T. A. Aung, N. Kaplowitz, C. García-Ruiz, and J. C. Fernández-Checa. 2019. Endoplasmic Reticulum Stress-Induced Upregulation of STARD1 Promotes Acetaminophen-Induced Acute Liver Failure. *Gastroenterology* 157, 552-568.
  21. Willenbring, H., and M. Grompe. 2013. A therapy for liver failure found in the JNK yard. *Cell* 153: 283–284.
  22. Ji, X. F., X. Y. Li, Y. C. Fan, Z. H. Zhao, S. Gao, F. K. Sun, J. Zhao, and K. Wang. 2015. Serum wnt5a is a predictor for the prognosis of acute on chronic hepatitis B liver failure. *Biomarkers: biochemical indicators of exposure, response, and susceptibility to chemicals* 20, 26-34.
  23. Maes, M., M. Vinken, and H. Jaeschke. 2016. Experimental models of hepatotoxicity related to acute liver failure. *Toxicology and applied pharmacology* 290: 86–97.
  24. Antoniadis, C. G., P. A. Berry, J. A. Wendon, and D. Vergani. 2008. The importance of immune dysfunction in determining outcome in acute liver failure. *Journal of hepatology* 49: 845–861.
  25. Rutherford, A., and R. T. Chung. 2008. Acute liver failure: mechanisms of hepatocyte injury and regeneration. *Seminars in liver disease* 28: 167–174.
  26. Farghali, H., M. Kgalalelo Kemelo, L. Wojnarová, and N. Kutinová Canová. 2016. In vitro and in vivo experimental hepatotoxic models in liver research: applications to the assessment of potential hepatoprotective drugs. *Physiological research* 65: S417–Ss425.
  27. Zhong, W., K. Qian, J. Xiong, K. Ma, A. Wang, and Y. Zou. 2016. Curcumin alleviates lipopolysaccharide induced sepsis and liver failure by suppression of oxidative stress-related inflammation via PI3K/AKT and NF- $\kappa$ B related signaling. *Biomedicine & pharmacotherapy = Biomedecine & pharmacotherapie* 83: 302–313.
  28. Galanos, C., M. A. Freudenberg, and W. Reutter. 1979. Galactosamine-induced sensitization to the lethal effects of endotoxin. *Proceedings of the National Academy of Sciences of the United States of America* 76: 5939–5943.
  29. Sen, M., K. Lauterbach, H. El-Gabalawy, G. S. Firestein, M. Corr, and D. A. Carson. 2000. Expression and function of wingless and frizzled homologs in rheumatoid arthritis. *Proceedings of the National Academy of Sciences of the United States of America* 97: 2791–2796.

30. Baarsma, H. A., W. Skronska-Wasek, K. Mutze, F. Ciolek, D. E. Wagner, G. John-Schuster, K. Heinzelmann, A. Günther, K. R. Bracke, M. Dagouassat, J. Boczkowski, G. G. Brusselle, R. Smits, O. Eickelberg, A. Yildirim, and M. Königshoff. 2017. Noncanonical WNT-5A signaling impairs endogenous lung repair in COPD. *The Journal of experimental medicine* 214: 143–163.
31. Bodmer, D., S. Levine-Wilkinson, A. Richmond, S. Hirsh, and R. Kuruvilla. 2009. Wnt5a mediates nerve growth factor-dependent axonal branching and growth in developing sympathetic neurons. *The Journal of neuroscience: the official journal of the Society for Neuroscience* 29: 7569–7581.
32. Baarsma, H. A., M. Königshoff, and R. Gosens. 2013. The WNT signaling pathway from ligand secretion to gene transcription: molecular mechanisms and pharmacological targets. *Pharmacology & therapeutics* 138: 66–83.
33. Tang, X., Y. Wu, T. Y. Belenkaya, Q. Huang, L. Ray, J. Qu, and X. Lin. 2012. Roles of N-glycosylation and lipidation in Wg secretion and signaling. *Developmental biology* 364: 32–41.
34. Li, P., Y. Cao, Y. Li, L. Zhou, X. Liu, and M. Geng. 2014. Expression of Wnt-5a and  $\beta$ -catenin in primary hepatocellular carcinoma. *International journal of clinical and experimental pathology* 7: 3190–3195.
35. Jenei, V., V. Sherwood, J. Howlin, R. Linnskog, A. Säfholm, L. Axelsson, and T. Andersson. 2009. A t-butyloxycarbonyl-modified Wnt5a-derived hexapeptide functions as a potent antagonist of Wnt5a-dependent melanoma cell invasion. *Proceedings of the National Academy of Sciences of the United States of America* 106: 19473–19478.
36. Li, X., J. Wen, Y. Dong, Q. Zhang, J. Guan, F. Liu, T. Zhou, Z. Li, Y. Fan, and N. Wang. 2021. Wnt5a promotes renal tubular inflammation in diabetic nephropathy by binding to CD146 through noncanonical Wnt signaling. *Cell death & disease* 12: 92.
37. Kikuchi, A., H. Yamamoto, A. Sato, and S. Matsumoto. 2012. Wnt5a: its signalling, functions and implication in diseases. *Acta physiologica (Oxford, England)* 204: 17–33.
38. Sun, M., W. Wang, L. Min, C. Chen, Q. Li, and W. Weng. 2021. Secreted frizzled-related protein 5 (SFRP5) protects ATDC5 cells against LPS-induced inflammation and apoptosis via inhibiting Wnt5a/JNK pathway. *Journal of orthopaedic surgery and research* 16: 129.
39. Yu, T., D. Dong, J. Guan, J. Sun, M. Guo, and Q. Wang. 2020. Alprostadil attenuates LPS-induced cardiomyocyte injury by inhibiting the Wnt5a/JNK/NF- $\kappa$ B pathway. *Herz* 45: 130–138.
40. Guha, M., and N. Mackman. 2001. LPS induction of gene expression in human monocytes. *Cellular signalling* 13: 85–94.
41. Lou, G., A. Li, Y. Cen, Q. Yang, T. Zhang, J. Qi, Z. Chen, and Y. Liu. 2021. Selonsertib, a potential drug for liver failure therapy by rescuing the mitochondrial dysfunction of macrophage via ASK1-JNK-DRP1 pathway. *Cell & bioscience* 11: 9.
42. Henderson, N. C., K. J. Pollock, J. Frew, A. C. Mackinnon, R. A. Flavell, R. J. Davis, T. Sethi, and K. J. Simpson. 2007. Critical role of c-jun (NH2) terminal kinase in paracetamol-induced acute liver failure. *Gut* 56: 982–990.

43. Yamaguchi, T. P., A. Bradley, A. P. McMahon, and S. Jones. 1999. A Wnt5a pathway underlies outgrowth of multiple structures in the vertebrate embryo. *Development (Cambridge, England)* 126: 1211–1223.

## Figures

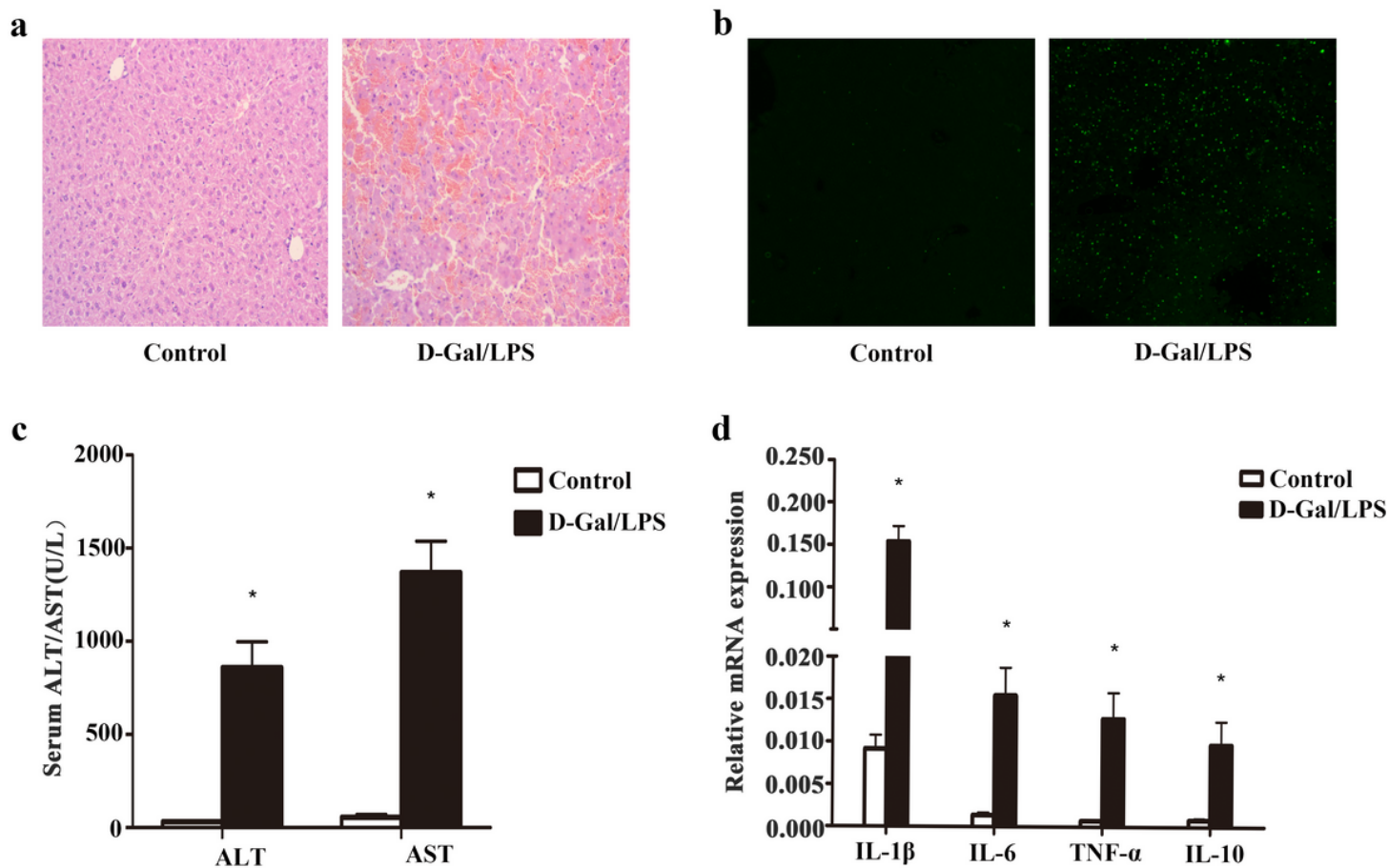


**Figure 1**

Hepatic damage was caused by D-Gal/LPS administration. a Histology of liver sections stained with H&E (magnification,  $\times 200$ ). Bar=100 $\mu$ m. b Cells apoptosis in liver sections using TdT-mediated dUTP Nick-End Labeling (TUNEL) staining (magnification,  $\times 100$ ). Bar=200 $\mu$ m. c Serum levels of alanine aminotransferase (ALT) and aspartate aminotransferase (AST). d Relative liver mRNA levels of tumor necrosis  $\alpha$  (TNF- $\alpha$ ), Interleukin-6 (IL-6), Interleukin-1 $\beta$  (IL-1 $\beta$ ) and Interleukin-10 (IL-10). Data are shown as mean  $\pm$  standard error of mean (SEM). n=10.\*P $\leq$ 0.05.

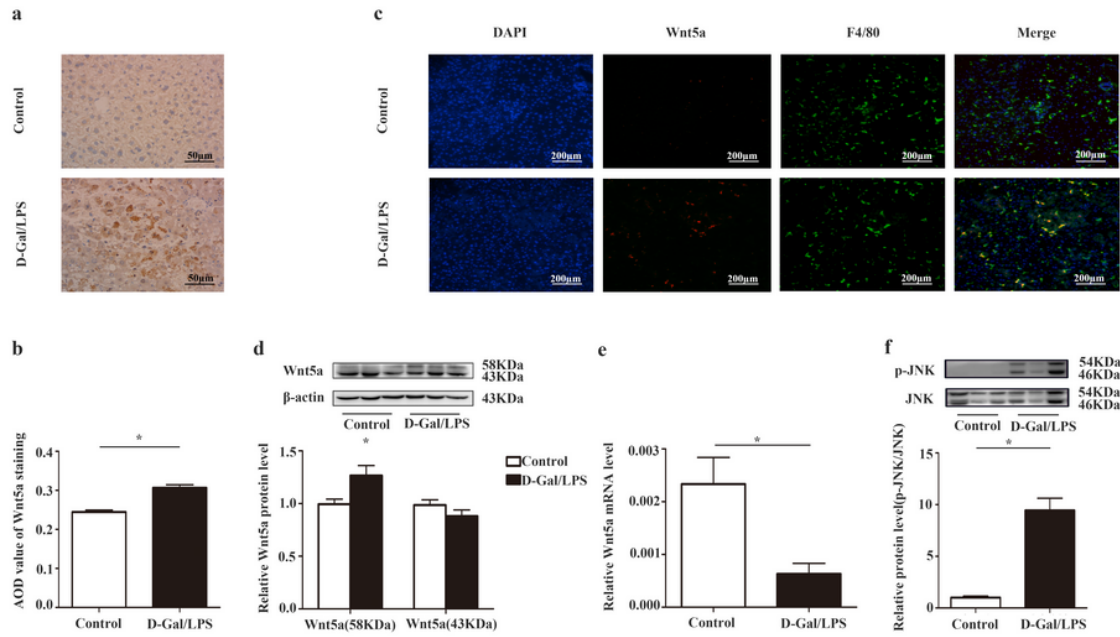


**Figure 2**

Aberrant Wnt5a expression and JNK activation in liver tissues were induced by D-Gal/LPS. a Representative immunohistochemistry photographs for Wnt5a (magnification,  $\times 400$ ). Bar=50 $\mu$ m. b Quantitative analysis of Wnt5a immunohistochemistry staining. c Representative immunofluorescence photographs for Wnt5a, F4/80 and DAPI (magnification,  $\times 100$ ). Bar=200 $\mu$ m. d Wnt5a protein levels by Western blot analysis. e Relative quantities of Wnt5a mRNA levels. f Assessment of JNK activation by Western blot analysis. Data are shown as mean  $\pm$  standard error of mean (SEM). n=10.\* $P < 0.05$

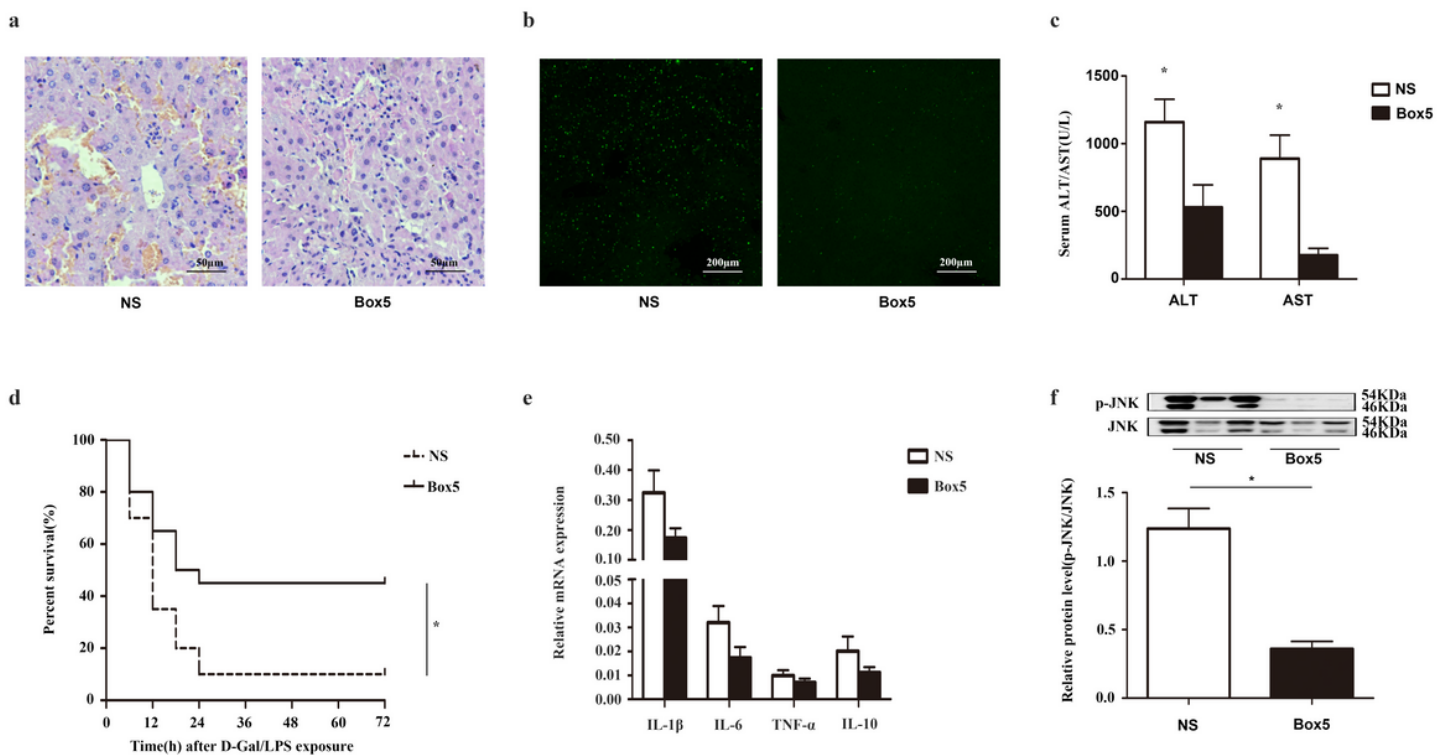


**Figure 3**

Box5 attenuated hepatic damage and reversed JNK activation. a Histology of liver sections stained with H&E (magnification,  $\times 400$ ). Bar=50 $\mu$ m. b Cells apoptosis in liver sections using TdT-mediated dUTP Nick-End Labeling (TUNEL) staining (magnification,  $\times 100$ ). Bar=200 $\mu$ m. c Serum levels of alanine aminotransferase (ALT) and aspartate aminotransferase (AST). d Survival rate within 72 h after D-Gal/LPS administration. e Relative quantities of mRNA levels, including tumor necrosis  $\alpha$  (TNF- $\alpha$ ), Interleukin-6 (IL-6), Interleukin-1 $\beta$  (IL-1 $\beta$ ) and Interleukin-10 (IL-10). f Assessment of JNK activation by Western blot analysis. Data are shown as mean  $\pm$  standard error of mean (SEM). n=10.\*P $\leq$ 0.05.

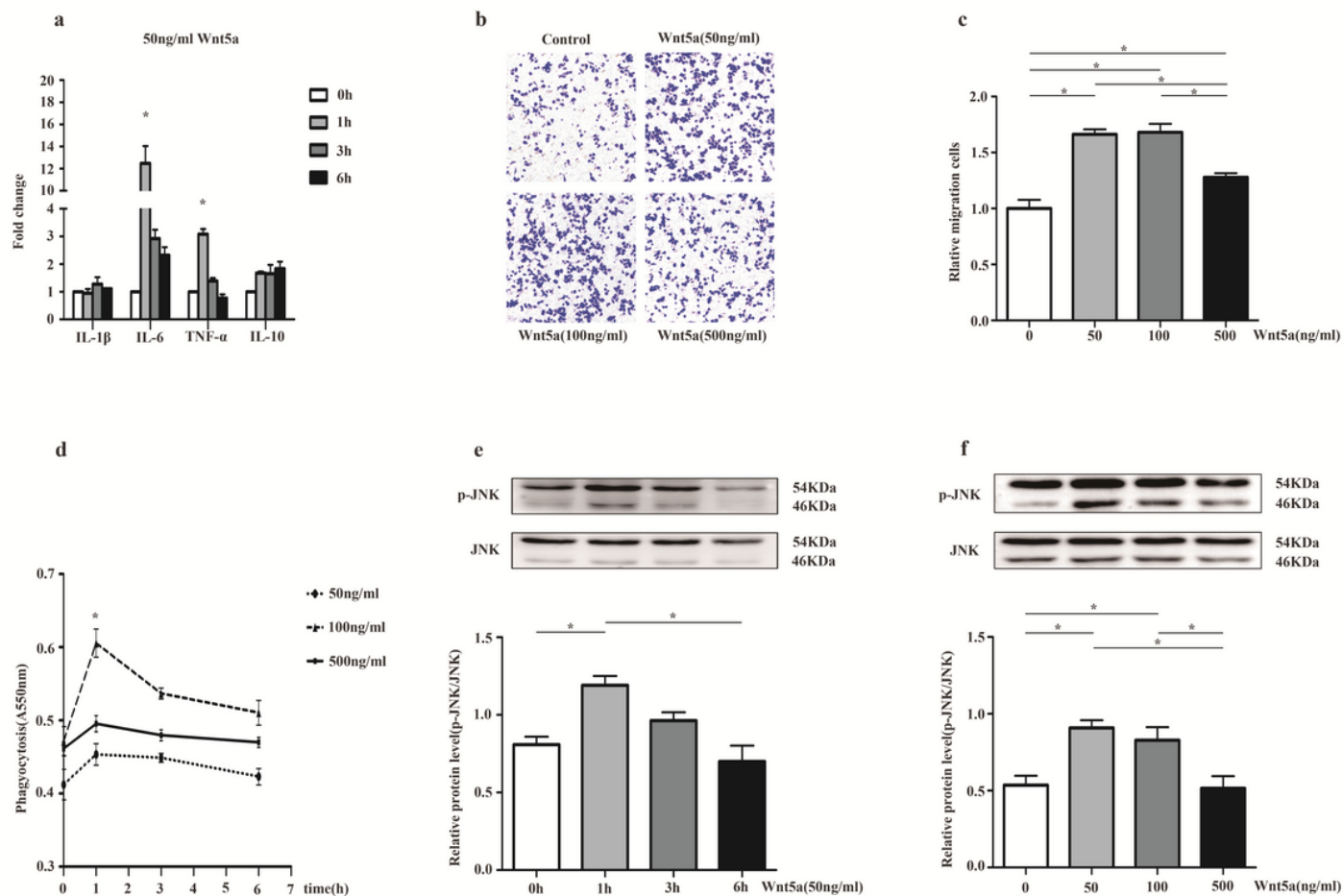


**Figure 4**

Recombinant Wnt5a (rWnt5a) induced downstream regulation, migration and phagocytosis of THP-1 macrophages. a Relative mRNA levels of tumor necrosis  $\alpha$  (TNF- $\alpha$ ), Interleukin-6 (IL-6), Interleukin-1 $\beta$  (IL-1 $\beta$ ) and Interleukin-10 (IL-10) in THP-1 macrophages treated by 50ng/ml rWnt5a for 1, 3, 6 h. b Transwell migration assay for THP-1 macrophages treated with different concentrations of rWnt5a (50, 100, 500ng/ml) for 24h (magnification,  $\times 200$ ). c Quantification analysis of migratory cells in five fields counted using Image J. d Neutral red uptake assay for THP-1 macrophages exposed to different concentrations of rWnt5a (50, 100, 500ng/ml) for 1, 3, 6 h. The absorbance at a wavelength of 550nm (A550nm) represented phagocytosis of THP-1 macrophages. e Assessment of JNK activation in THP-1 macrophages treated by 50ng/ml rWnt5a for 1, 3, 6 h using Western blot. f Assessment of JNK activation in THP-1 macrophages treated by rWnt5a with 50, 100, 500ng/ml using Western blot. Data are shown as mean  $\pm$  standard error of mean (SEM). \* $P < 0.05$ .

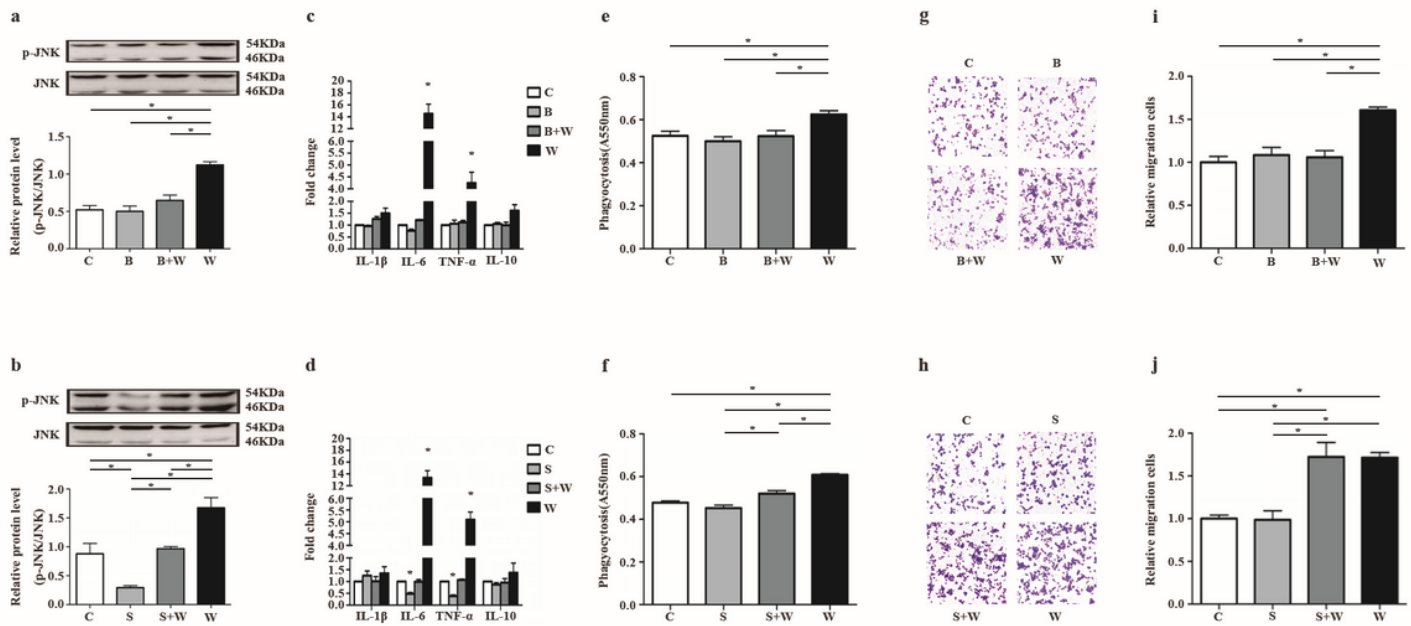


**Figure 5**

Box5 and SP600125 reversed the most effects exerted by rWnt5a on THP-1 macrophages. JNK activation (a, b) and relative mRNA levels of inflammatory cytokines (c, d) were assessed in THP-1 macrophages treated with 50ng/ml rWnt5a for 1h with or without 200 $\mu$ M Box5 or 40nM SP600125. Neutral red uptake assay was conducted to evaluate the phagocytosis of THP-1 macrophages treated with 100ng/ml rWnt5a for 1h with or without 200 $\mu$ M Box5 (e) or 40nM SP600125 (f). The absorbance at a wavelength of 550nm (A550nm) represented phagocytosis of THP-1 macrophages. Transwell migration assay (g, h) and quantification analysis (i, j) was used to analyze the migratory THP-1 macrophages treated with 50ng/ml rWnt5a for 24h with or without 200 $\mu$ M Box5 or 40nM SP600125 (magnification,  $\times$ 200). C, Control; B, Box5; S, SP600125; B+W, Box5 + rWnt5a; S+W, SP600125+rWnt5a; W, rWnt5a. Data are shown as mean  $\pm$  standard error of mean (SEM). \* $P$  $\leq$ 0.05.